Low-temperature fabrication of carbon nanofibers by self-assembling of polycyclic aromatic hydrocarbon molecules

Shich-Chang Suen, Wha-Tzong Whang, Bo-Wei Wu, and Yi-Fan Lai
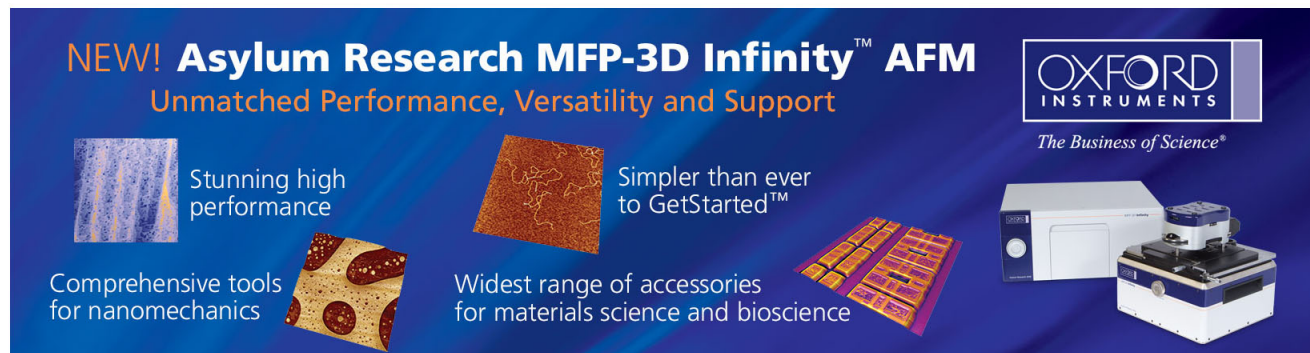
Articles you may be interested in

Large area orientation films based on graphene oxide self-assembly and low-temperature thermal reduction
Appl. Phys. Lett. **101**, 181903 (2012); 10.1063/1.4764549

A simple method to prepare self-assembled organic-organic heterobilayers on metal substrates
AIP Advances **1**, 022112 (2011); 10.1063/1.3591389

Phase change nanodot arrays fabricated using a self-assembly diblock copolymer approach
Appl. Phys. Lett. **91**, 013104 (2007); 10.1063/1.2753699

Ion-assisted precursor dissociation and surface diffusion: Enabling rapid, low-temperature growth of carbon nanofibers
Appl. Phys. Lett. **90**, 251501 (2007); 10.1063/1.2750392

Room-temperature growth of a carbon nanofiber on the tip of conical carbon protrusions
Appl. Phys. Lett. **84**, 3831 (2004); 10.1063/1.1745109

Low-temperature fabrication of carbon nanofibers by self-assembling of polycyclic aromatic hydrocarbon molecules

Shich-Chang Suen and Wha-Tzong Whang[a]
Department of Materials Science and Engineering, National Chiao Tung University, 1001 Ta Hsueh Road, Hsinchu 30050, Taiwan, Republic of China

Bo-Wei Wu and Yi-Fan Lai
National Nano Device Laboratories, 1001-1 Ta Hsueh Road, Hsinchu 30050, Taiwan, Republic of China

Carbon nanofibers (CNFs) with diameter ~66 nm have been synthesized from coronene by low-temperature (~45 °C) vacuum sublimation without the aid of a catalyst. Our method makes use of the property of polycyclic aromatic hydrocarbon (PAH) molecules, which can self-assemble into columnar aggregates. This polycyclic aromatic hydrocarbon-carbon nanofibers (PAH-CNFs) reveal much better thermal stability than commercial carbon nanotubes and exhibit field-emission characteristics with the onset of an electric field of 5.4 V/μm and field enhancement factor of 1326 cm^{-1} for 100 μm interelectrode distance. The relative high thermal stability and easier process open up a possibility to fabricate large-scale field-emission devices in an efficient way and to provide a broad range of applications in nanoscience and technology. © *2004 American Institute of Physics.*
[DOI: 10.1063/1.1707229]

Recently, one-dimensional (1-D) carbonaceous nanostructures, such as tubes, fibers, wires, and rods, have become the focus of intensive research owing to their unique applications in nanoscale devices. For example, carbon nanotubes (CNTs) could act as tips of a scanning probe microscope,[1] field emitters in flat panel displays,[2] single-molecular transistors,[3] quantum wires,[4] and electron emitters for generating x rays.[5]

Various methods to synthesize 1-D carbonaceous nanostructures have been brought up by many research groups. Arc discharge,[6] laser ablation,[7] pyrolysis,[8] and catalytic decomposition of hydrocarbons[9] were common methods to produce CNTs or carbon nanofibers (CNFs). Both the arc and laser ablation were inadequate on the point of view of large-scale production. The catalytic decomposition method has seemed to be the most promising one at present owing to the lower investment cost and lower reaction temperature (650 °C).

To date, the lowest temperature at which to fabricate CNTs through the catalytic decomposition method is about 400 °C, with the assistance of plasma-enhanced chemical vapor deposition (PECVD).[10] However, the expensive equipment and confined deposition area limited by electrode size make this process hard to scale up.

In this study, an easier way was suggested to produce a 1-D carbonaceous nanostructure. By utilizing the π–π interaction between polycyclic aromatic hydrocarbon (PAH) molecules, which can self-assemble into columnar aggregates,[11] CNFs with a diameter of ~66 nm can be fabricated directly by vacuum sublimation of PAH molecules. This process proceeded without the aid of a catalyst and high temperature. The results of this study could be very useful to produce CNF-related devices in great quantities.

Using coronene, one kind of PAH molecule, as a starting material, PAH-CNFs were fabricated on a gold substrate by vacuum sublimating coronene from a heated crucible (~45 °C) at a deposition rate of ~6 Å/min. The gold substrate was kept at room temperature and a background pressure around 3×10^{-6} Torr. Structural investigations were carried out in a Joel JSM-6500F scanning electron microscope (SEM). Contact angles and surface free energies were determined using a KRÜSS universal surface tester (model GH-100). Thermal stability was evaluated by Hitachi thermal desorption system-atmospheric pressure ionization mass spectrometer (TDS-APIMS).

Figure 1 shows SEM images of PAH-CNFs deposited by vacuum sublimation for 90 min. The fibers were nearly vertically grown on gold substrate with a uniform average density of 10^8/cm^2, which is slightly less than that of CNTs synthesized by Ni-catalyzed PECVD process ($\sim 10^9$/cm^2).[12] The mean diameter of fibers was around 66 nm calculated from the diameter histogram, which was based on the SEM
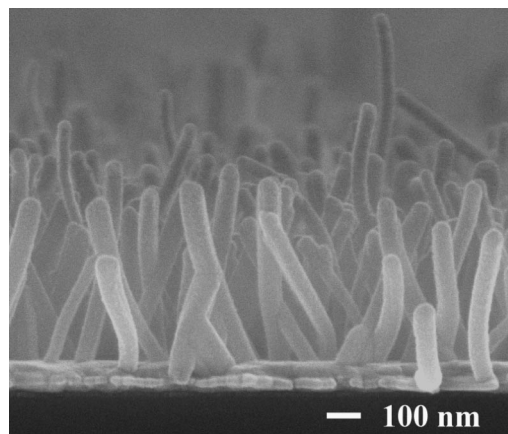

FIG. 1. Cross-sectional SEM image of PAH-CNFs deposited by vacuum sublimation for 90 min.

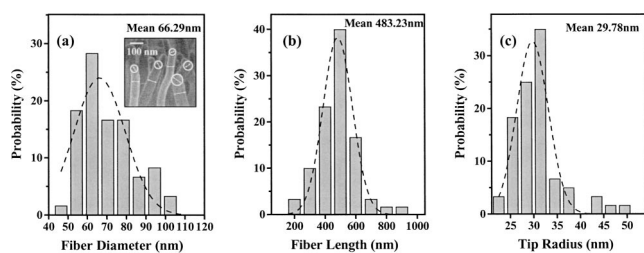[a]Electronic mail: wtwhang@mail.NCTU.edu.tw

FIG. 2. Histograms of (a) fiber diameter, (b) fiber length, and (c) tip radius of PAH-CNFs. Inset demonstrated the way to measure tip radius from SEM image.

images of PAH-CNFs, as shown in the inset of Fig. 2(a). Figures 2(b) and 2(c) show the histograms of fiber length and tip radius, respectively. The fiber lengths ranged from 0.2 to 1 μm and the mean length was about 483 nm. Instead of extending the deposition time, but rather to increase the deposition rate in a shorter process time, fibers longer than 3 μm can be obtained. The tip radius was determined by placing an approximate circle on each tip in SEM images then measured radius of each circle. The tip radius, which will characterize the field emission, ranged from 10 to 50 nm, and the mean value was 30 nm.

The growth mechanism was different from catalytic decomposition method that normally involves three steps: (i) decomposition of hydrocarbon reactants on catalyst surface; (ii) forming a supersaturated solution of carbon and catalyst; and (iii) precipitation of carbon which extrudes the walls.[13,14] Since no catalyst or heating process were involved in our experiment, the growth of PAH-CNFs was not by way of decomposition and rearrangement of coronene.

For aromatic hydrocarbons, which possess large polarizabilities and small local dipole moments, the dispersion interaction would attract molecules to stack in column.[11,15] However, the repulsive force among nuclei may lead to a parallel-displaced conformation resulting in a tilted columnar structure.[15] The same situation was found in Fig. 1, the fiber growing direction was nearly vertically aligned, but slightly tilted at an angle of 5°–10° away from verticality.

Besides the dispersion force, the surface energy of substrate, which relates to the unsaturated surface bond, also affects the geometry of PAH-CNFs. Figure 3 shows top-view SEM images of PAH-CNFs on (a) gold substrate and (b) silicon dioxide substrate. The fibers on gold substrate stood up straight, however, those on silicon dioxide surface lay down and entangled in the majority. The better wettability of silicon dioxide might due to the higher concentration of unsaturated surface bonds, which tend to adsorb molecules to lower the surface free energy. This is consistent with our
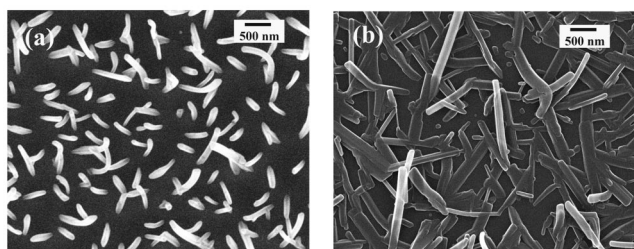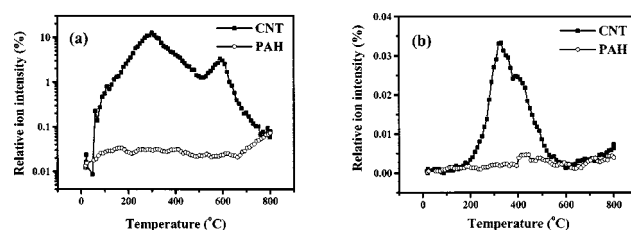

FIG. 4. Thermal desorption curve of (a) CO_2 ($m/z = 44$) and (b) C_6H_6 ($m/z = 78$) for both CNTs and PAH-CNFs.

results on contact angle measurement. The surface free energy was 40 mJ/m^2 for gold substrate and 49 mJ/m^2 for silicon dioxide substrate. These values were calculated by the Owens method from the measured contact angles for three different solvents (diiodo methane, ethylene glycol, and water) on each substrate. As coronene molecules deposit on silicon dioxide, the π–π interaction still holds discotic molecules together, however the existing of π-surface bonds results in an edge-on morphology rather than a face-on morphology.[16]

Thermal stability is a crucial property to evaluate feasibility for applying a new material in use. TDS-APIMS was used here to monitor thermal desorption behavior of PAH-CNFs by heating the sample from 25 up to 800 °C at a ramp rate of 10 °C/min. For comparison, the same-sized-area CNT films deposited by electrophoresis[17] was measured under the same conditions. Figure 4(a) shows the CO_2 ($m/z = 44$) desorption curve of both PAH-CNFs and CNTs, revealing that PAH-CNFs are very stable for less carbonaceous species, which are oxidized and desorbed as CO_2 for PAH-CNFs, which is no the case for CNTs. The better thermal stability of PAH-CNFs can be further confirmed by the much lower desorption of benzene species C_6H_6 ($m/z = 78$), as shown in Fig. 4(b). The superior thermal stability might be attributed to the chemically perfect π-delocalization in these seven aromatic rings of coronene, which consequently offers stronger C–C bonds. Despite the fact that CNTs possess a similar structure, the unexpected structural defect that arose during synthesis (e.g., saturated C–C bond or open rings) will degrade the structural stability. In addition, the amorphous porous carbon[18] congested among the tubes or the residues from electrophoresis process also results in the larger desorption of CO_2 for CNTs. The thermal decomposition occurred above 600 °C of PAH-CNFs was similar with the results of other reports for CNTs.[9,18,19]

Field emission of PAH-CNFs was measured by placing a cylindrical electrode of 2.2 mm diameter above the fibers surface at a distance of 100 μm. All the measurements were carried out in a vacuum chamber under a pressure of 10^{-6} Torr, with Keithley 237 as a power supplier, and a current meter. Figure 5 shows a typical plot of the emission current density J versus the applied field E. The onset field for producing a current density of 10 μA/cm^2 was near 5.4 V/μm. This result is similar with a CNT array ($\sim$5.5 V/μm)[20] measured with the same method. The inset in Fig. 5 reveals J–E characteristics for PAH-CNFs that followed Fowler–Nordheim (FN) behavior. After a well-defined FN-type threshold field, there is an exponential current rise region, followed by saturation. This saturation, which occurred at high voltage, might result from the deficiency of emitting electrons that happened owing to the burning out of emitting
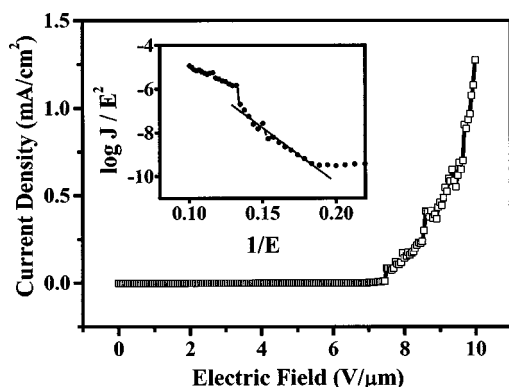

FIG. 3. Top-view SEM images of PAH-CNFs on (a) gold substrate and (b) silicon dioxide substrate.

FIG. 5. Field-emission J–E curve of PAH-CNFs. Inset: corresponding FN plot.

tips[21] or the saturated drift velocity of carriers in the fibers.[22] Because PAH-CNFs were constructed by superposing PAH molecules layer by layer, the electrons were transported across molecules under the bias of an electric field. Normally, intermolecular transporting is slower than intramolecular transporting, so that the limited drift velocity might be the reason for current saturation.

The field enhancement factor β is defined as $\beta = F/E$, where F is the effective electric field at the surface of tip and E is the applied electric field. Taking the tip work function to be that of graphite ($\sim$5 eV), which applies to most case of CNTs,[23] the field enhancement factor β could be deduced from the slope of fitting line, which was approximately 1326 cm^{-1}, analogous to the value of CNT films (1000–3000 for 125 μm interelectrode distance).[23] Normally, β is inversely proportional to the tip radius in the concept of electrostatic properties.[24] The larger radius of PAH-CNFs ($\sim$30 nm), as compared with a multiwalled nanotube tip ($\sim$4 nm),[25] resulted in a smaller β value that caused a higher onset of an electric field. Moreover, from our recent data, we observed the longer PAH-CNFs needed a higher electric field to produce the same current density as the shorter one. The certain resistance raised from the slower intermolecular electron transporting might also be responsible to the higher onset electric field.

In summary, by utilizing coronene as a starting material, carbon nanofibers were deposited simply by low-temperature ($\sim$45 °C) vacuum evaporation without the help of a catalyst and high temperature. The nearly vertical growing PAH-CNFs on gold substrate were dominated by π–π interaction and surface energy. This PAH-CNFs reveal much better thermal stability than commercial CNTs. They also exhibit field-emission characteristics and follow Fowler–Nordheim behavior, as do the CNTs. The relative high thermal stability and easier process provide a broad range of applications in nanoscience and technology.

[1] H. Dai, J. H. Hafner, A. G. Rinzler, D. T. Colbert, and R. E. Smalley, Nature (London) **384**, 147 (1996).
[2] W. A. de Heer, W. S. Bacsa, A. Châtelain, T. Gerfin, R. Humphrey-Baker, L. Forró, and D. Ugarte, Science **268**, 845 (1995).
[3] S. J. Tans, A. R. M. Verschueren, and C. Dekker, Nature (London) **393**, 49 (1998).
[4] S. J. Tans, M. H. Devoret, H. Dai, A. Thess, R. E. Smalley, L. J. Geerligs, and C. Dekker, Nature (London) **386**, 474 (1997).
[5] G. Z. Yue, Q. Qiu, B. Gao, Y. Cheng, J. Zhang, H. Shimoda, S. Chang, J. P. Lu, and O. Zhou, Appl. Phys. Lett. **81**, 355 (2002).
[6] C. Journet, W. K. Maser, P. Bernier, A. Loiseau, M. Lamy de la Chapelle, S. Lefrant, P. Deniard, R. Lee, and J. E. Fischer, Nature (London) **388**, 756 (1997).
[7] A. Thess, R. Lee, P. Nikolaev, H. Dai, P. Petit, J. Robert, C. Xu, Y. H. Lee, S. G. Kim, A. G. Rinzler, D. T. Colbert, G. E. Scuseria, D. Tománek, J. E. Fisher, and R. E. Smalley, Science **273**, 483 (1996).
[8] M. Terrones, N. Grobert, J. Olivares, J. P. Zhang, H. Terrones, K. Kordatos, W. K. Hsu, J. P. Hare, P. D. Townsend, K. Prassides, A. K. Cheetham, H. W. Kroto, and D. R. M. Walton, Nature (London) **388**, 52 (1997).
[9] Y. Yang, Z. Hu, Y. J. Tian, Y. N. Lü, X. Z. Wang, and Y. Chen, Nanotechnology **14**, 733 (2003).
[10] Y. Shiratori, H. Hiraoka, Y. Takeuchi, S. Itoh, and M. Yamamoto, Appl. Phys. Lett. **82**, 2485 (2003).
[11] A. M. van de Craats, J. M. Warman, K. Müllen, Y. Geerts, and J. D. Brand, Adv. Mater. (Weinheim, Ger.) **10**, 36 (1998).
[12] K. B. K. Teo, M. Chhowalla, G. A. J. Amaratunga, W. I. Milne, G. Pirio, P. Legagneux, F. Wyczisk, D. Pribat, and D. G. Hasko, Appl. Phys. Lett. **80**, 2011 (2002).
[13] V. I. Merkulov, M. A. Guillorn, D. H. Lowndes, M. L. Simpson, and E. Voelkl, Appl. Phys. Lett. **79**, 1178 (2001).
[14] V. Vinciguerra, F. Buonocore, G. Panzera, and L. Occhipinti, Nanotechnology **14**, 655 (2003).
[15] J. D. Wright, *Molecular crystals*, 2nd ed. (Cambridge University Press, Cambridge, UK, 1995), p. 22.
[16] R. Hurt, G. Krammer, G. Crawford, K. Jian, and C. Rulison, Chem. Mater. **14**, 4558 (2002).
[17] W. B. Choi, Y. W. Jin, H. Y. Kim, S. J. Lee, M. J. Yun, J. H. Kang, Y. S. Choi, N. S. Park, N. S. Lee, and J. M. Kim, Appl. Phys. Lett. **78**, 1547 (2001).
[18] W. Q. Han, W. Mickelson, J. Cumings, and A. Zettl, Appl. Phys. Lett. **81**, 1110 (2002).
[19] Y. C. Sui, D. R. Acosta, J. A. González-León, A. Bermúdez, J. Feuchtwanger, B. Z. Cui, J. O. Flores, and J. M. Saniger, J. Phys. Chem. B **105**, 1523 (2001).
[20] Y. H. Wang, J. Lin, and C. H. A. Huan, Thin Solid Films **405**, 243 (2002).
[21] I. Alexandrou, M. Baxendale, N. L. Rupesinghe, G. A. J. Amaratunga, and C. J. Kiely, J. Vac. Sci. Technol. B **18**, 2698 (2000).
[22] M. Ding, H. Kim, and A. I. Akinwande, Appl. Phys. Lett. **75**, 823 (1999).
[23] J. M. Bonard, J. P. Salvetat, T. Stöckli, W. A. de Heer, L. Forró, and A. Châtelain, Appl. Phys. Lett. **73**, 918 (1998).
[24] M. A. Guillorn, A. V. Melechko, V. I. Merkulov, D. K. Hensley, M. L. Simpson, and D. H. Lowndes, Appl. Phys. Lett. **81**, 3660 (2002).
[25] J. M. Bonard, F. Maier, T. Stöckli, A. Châtelain, W. A. de Heer, J. P. Salvetat, and L. Forró, Ultramicroscopy **73**, 7 (1998).